

University of Texas Rio Grande Valley

ScholarWorks @ UTRGV

School of Podiatric Medicine Publications and
Presentations

School of Podiatric Medicine

2-2020

Investigation of the early healing response to dicationic imidazolium-based ionic liquids: a biocompatible coating for titanium implants

Sutton E. Wheelis

University of Texas at Dallas

Cláudia Cristina Biguetti

The University of Texas Rio Grande Valley, claudia.biguetti@utrgv.edu

Shruti Natarajan

Lidia Guida

Brian Hedden

See next page for additional authors

Follow this and additional works at: https://scholarworks.utrgv.edu/sopm_pub



Part of the [Medicine and Health Sciences Commons](#)

Recommended Citation

Wheelis, S. E., Biguetti, C. C., Natarajan, S., Guida, L., Hedden, B., Garlet, G. P., & Rodrigues, D. C. (2020). Investigation of the early healing response to dicationic imidazolium-based ionic liquids: a biocompatible coating for titanium implants. *ACS biomaterials science & engineering*, 6(2), 984–994. <https://doi.org/10.1021/acsbomaterials.9b01884>

This Article is brought to you for free and open access by the School of Podiatric Medicine at ScholarWorks @ UTRGV. It has been accepted for inclusion in School of Podiatric Medicine Publications and Presentations by an authorized administrator of ScholarWorks @ UTRGV. For more information, please contact justin.white@utrgv.edu, william.flores01@utrgv.edu.

Authors

Sutton E. Wheelis, Cláudia Cristina Biguetti, Shruti Natarajan, Lidia Guida, Brian Hedden, Gustavo P. Garlet, and Danieli C. Rodrigues



Published in final edited form as:

ACS Biomater Sci Eng. 2020 February 10; 6(2): 984–994. doi:10.1021/acsbiomaterials.9b01884.

Investigation of the early healing response to dicationic imidazolium-based ionic liquids: a biocompatible coating for titanium implants

Sutton E. Wheelis¹, Claudia C. Biguetti^{2,4}, Shruti Natarajan³, Lidia Guida¹, Brian Hedden¹, Gustavo P. Garlet⁴, Danieli C. Rodrigues^{1,*}

¹Department of Bioengineering, University of Texas at Dallas.

²Department of Basic Sciences, São Paulo State University (UNESP), School of Dentistry, Araçatuba, São Paulo, Brazil

³Department of Biological Sciences, University of Texas at Dallas.

⁴Bauru School of Dentistry, Department of Biological Sciences, University of São Paulo São Paulo, Brazil

Abstract

Dicationic Imidazolium-based ionic liquids with amino acid anions (IonL) have been proposed as a multifunctional coating for titanium dental implants, as their properties have been shown to address multiple early complicating factors while maintaining host cell compatibility. This study aims to evaluate effects of this coating on host response in the absence of complicating oral factors during the early healing period using a subcutaneous implantation model in the rat. IonLs with the best cytocompatibility and antimicrobial properties (IonL-Phe, IonL-Met) were chosen as coatings. Three different doses were applied to cpTi disks and subcutaneously implanted into 36 male Lewis rats. Rats received 2 implants: 1 coated implant on one side and an uncoated implant on the contralateral sides (n=3 per formulation, per dose). Peri-implant tissue was evaluated 2 and 14 days after implantation with H&E staining and IHC markers associated with macrophage

*Corresponding Author/Address: Dr. Danieli C. Rodrigues, Danieli@utdallas.edu, 800 W Campbell Rd. BSB11, Richardson TX 75080.

Author Addresses: Sutton E. Wheelis, Sutton.wheelis@utdallas.edu, 800 W Campbell Rd. BSB11, Richardson, TX 75080.

Claudia C. Biguetti, R. José Bonifácio, 1193 – Centro Araçatuba – SP, Brazil, 16011-071

Shruti Natarajan, Shruti.Natarajan@utdallas.edu, 800 W Campbell Rd., Richardson, TX 75080.

Lidia Guida, Lxg142030@utdallas.edu, 800 W Campbell Rd. BSB11, Richardson, TX 75080.

Brian Hedden, Hedden.brian@gmail.com, 800 W Campbell Rd., Richardson, TX 75080.

Dr. Gustavo P. Garlet, Alameda Doutor Octávio Pinheiro Brisola, 9-75, Bauru-SP, Brazil, 17012-901.

Author Contributions:

All authors have been selected based on their contributions to the conception, design of the work; or the acquisition, analysis or interpretation of data for the work; and drafting or revising the paper critically; and final approval of the version to be published. The authors listed agree to be accountable for aspects of the work in ensuring that questions related to the accuracy or integrity of any parts of the work are appropriately investigated and resolved.

Sutton E. Wheelis: Concept/Design, data collection/analysis/interpretation, and drafting article.

Dr. Claudia C. Biguetti: Concept/Design, data interpretation, and critical revision of article.

Shruti Natarajan: Data collection/analysis/interpretation.

Lidia Guida: Data collection/analysis/interpretation.

Brian Hedden: Data collection.

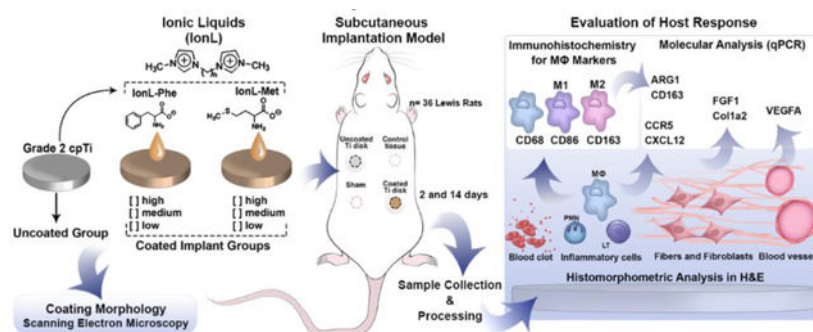
Dr. Gustavo P. Garlet: Concept/Design, critical revision of article.

Dr. Danieli C. Rodrigues*: Concept/Design, critical revision of article, and approval of article

Disclosures: The authors declare there are no conflicts of interest in this study.

polarization as well as molecular analysis (qPCR) for inflammatory and healing markers. H&E stains revealed the presence of the coating, blood clots and inflammatory infiltrate at 2 days around all implants. At 14 days, inflammation had receded with more developed connective tissue with fibroblasts, blood vessels in certain doses of coated and uncoated samples with no foreign body giant cells. This study demonstrated that IonL at the appropriate concentration does not significantly interfere with and healing and Ti foreign body response. Results regarding optimal dose and formulation from this study will be applied in future studies using an oral osseointegration model.

Graphical abstract



Keywords

Early Healing; Ionic Liquids; Titanium; Histology; Subcutaneous Implant; Multifunctional Coatings

1. Introduction

Commercially pure titanium (cpTi) and its alloys remain the most popular material utilized in dental implant fixtures due to the materials' favorable mechanical properties, corrosion resistance, and the ability to osseointegrate due to the materials' naturally forming oxide layer.^{1,2} The devices are considered successful, but implant failures are still reported at a rate from 1.9–11%.^{3–8} In an effort to better understand the nature of these failures, implant loss is categorized as an early or late failure.³ Early failures occur due to a lack of osseointegration around the implant, while late failures are caused by disruption of osseointegration.^{3,9} While there is an effort to mitigate both failures, late failures are difficult to treat in the clinic, and the attempts to revise these implants often result in a decreased likelihood of re-osseointegration.^{10,11} By placing an emphasis on early failures, clinicians maximize preventative measures to mitigate both early and late implant loss, as all types of implant failures are often preceded by an early loss.^{12,13} Early failures are often caused by several synergistic factors, such as surgical trauma, bacterial infiltration, or occlusal overload.^{3,14,15} Regardless of the cause, the result is often impaired healing due to an unbalanced and destructive inflammatory response, inhibiting osseointegration.^{16–18} Therefore, in order to increase chances for short and long-term success of dental implants, emphasis must be placed on maintaining the normal progression of inflammation and healing to establish stable osseointegration during the early healing period.

In general, titanium-based device placement is associated with a small degree of transitory inflammation, involving a balance between pro-inflammatory (M1) and regenerative (M2) macrophages during the host response, resulting in successful integration between the biomaterial and the host tissue.^{19–21} However, as mentioned above, a multitude of complications and failure modes associated with titanium implants have been reported in the literature, frequently associated with chronic and unbalanced inflammatory response.^{6,7,22,23} At this point, it is important to consider that the nature and intensity of the immune/inflammatory response of tissue interfacing with the biomaterial is the ultimate deciding factor on the successful healing outcome and maintenance of an implant.^{21,24} The presence of bacterial biofilms or trauma can disrupt the balance between titanium-tissue interactions. This interference can result in sustained and exacerbated inflammation, a foreign body reaction (FBR) and finally fibrotic encapsulation of a biomaterial or resorption of tissue, clinically translated as implant failure.^{25–28}

Surface modifications to titanium implants have attempted to directly address these complicating factors. In the clinic, modifications to the titanium oxide surface via sand blasted acid-etched surfaces (SLA) are utilized to improve bone and soft tissue cell attachment. In the literature, a wide array of approaches are explored: eliminating bacteria from the surface with silver nanoparticles, copper-bearing Ti alloys or antimicrobial coatings^{29,30} and encouraging mammalian bone and soft tissue attachment with porous or calcium phosphate coatings.^{31,32} These treatments can be effective, but each system or each modification described is only designed to address a specific complication, and often disregard the potential effects modifying surface properties can have on the FBR to an implant. Ideally, the next generation of surfaces would provide multifunctionality to address several potential complications that can impact early healing and functional integration, as well as encouraging a regenerative healing response.

In this context, recent efforts have been focused on investigating coatings to address multiple factors affecting surface performance, such as ionic liquids (IonLs).³³ IonLs are molten salts that have been widely used in industrial applications as lubricants or in the pharmaceutical industry as active ingredients.^{34–36} They are appealing for a range of applications because of their tunability, as cationic and anionic moieties and alkyl chain length of the molecule can be changed to suit a particular function.³³ In the interest of developing a coating for titanium implants, Gindri et al. proposed a dicationic imidazolium-based ionic liquid with amino acid anions.³³ The dicationic structure lowered the surfactant toxicity of the standard monocationic ionic liquid, by keeping the alkyl chain unexposed, and thought to improve biocompatibility by using amino acids as anions.^{33,37} Two formulations of these ionic liquids, with phenylalanine (IonL-Phe) and methionine (IonL-Met) anions exhibited several properties favorable for orthopedic and dental implant applications *in vitro*.^{33,37,38}

The key feature of the both IonL formulations (IonL-Phe and IonL-Met) was their selective toxicity to strains of bacteria known to constitute dental biofilms (*S. mutans*, *S. sanguinis*, and *S. salivarius*), while maintaining compatibility with bone and soft tissue forming cells, providing conditions for recovery and proliferation of bone and soft tissue cells in the absence of bacteria.^{33,39} However, only doses equal to or less than the IC₅₀ of both IonL

formulations had anti-microbial activity and maintained bone and soft-tissue cell compatibility, while higher doses were shown to be toxic to host cells *in vitro*.³³ In addition to their antimicrobial activity, IonL-Phe and IonL-Met were found to form a stable coating on titanium oxide resulting in anti-corrosive and lubricative properties, remaining on the surface for 7 days before releasing in solution.^{37–40} Although this coating has been extensively characterized, these previous results are limited by the scope of *in vitro* models, and there has been no investigation on how the presence of this coating affects the onset of inflammation and early healing outcomes *in vivo*. Thus, the purpose of this study is to evaluate, for the first time, the host biological response of IonL-Phe and IonL-Met coatings on titanium directly implanted subcutaneously in the connective tissue of rats, in the absence of external variables associated with the oral environment (bacteria, pH flux, saliva, and bolus). This sterile model is utilized in order to strictly assess the effect of the coating on the host response to titanium implants, and not its multifunctionality. Importantly, the subcutaneous compartment have been extensively used to address biocompatibility features of different biomaterials, and to be representative of host inflammatory immune response raised to implanted devices/materials. Results from this study will provide insight to most suitable formulation and amount of IonL to be evaluated in a more clinically relevant oral osseointegration model. It is hypothesized that a dose of IonL-Phe or IonL-Met below or equal to the IC₅₀ will maintain the biocompatibility of titanium necessary for tissue regeneration. Following implantation, the effect of both IonL on early healing was assessed using histological, histomorphometric and molecular characterization to evaluate coating impact on healing.

2. Materials and Methods

The two IonL utilized in this study: 1,10-bis(3-methylimidazolium-1-yl)decane diphenylalanine (IonL-Phe), and 1,10-bis(3-methylimidazolium-1-yl)decanedimethionine (IonL-Met) were synthesized based on a method proposed by Fukumoto et al. using protocols previously established in the literature.^{33,41} Both IonLs were characterized using ¹H and ¹³C nuclear magnetic resonance spectrometry to verify structure with existing literature, shown in Figure 1³³.

2.1 Sample Preparation

Grade 2 cpTi (3 mm \varnothing \times 2 mm, McMaster Carr, Elmhurst, IL, USA) polished with 240 grit silica paper were used as subcutaneous implants in this study. All implants were cleaned by sonicating for 45 min each in acetone, DI water, and ethanol solutions, respectively. After sonication, implants were dried in the oven at 65 °C overnight and finally sterilized in an autoclave. Experimental samples receiving the ionic liquid coating were dip coated in varied concentrations of ethanolic IonL-Phe or IonL-Met solutions for 10 minutes to achieve 3 different doses denoted low, medium and high, shown in Table 1. Characterizations of these coatings on titanium have been performed in previous studies, but scanning electron microscopy in high vacuum mode (SEM, JEOL SM-6010LA, Jeol Peabody, MA) was used to visualize the coating morphology at the three different doses per coating in this study³⁷. Previous studies have reported that the IC₅₀ of both IonL-Phe and IonL-Met are 8.5 ± 1.5 mM and 13.9 ± 2.7 mM respectively, corresponding to approximately 0.85 μ mol of IonL-

Phe and 1.39 μmol of IonL-Met in contact with cells^{33,39}. In order to understand the impact of IonL dose on the immune response and wound healing *in vivo*, different doses of ionic liquid both above and below to the previously observed *in vitro* IC_{50} were used in this study, as listed in Table 1. After 10 minutes in the ethanolic IonL solution, implants were removed from the solution at a uniform rate of 60 $\mu\text{m}/\text{sec}$ with the assistance of a motorized stage (TA Instruments, New Castle, DE, USA) then placed in an oven at 65 °C to dry for 48 hours. To achieve the desired coating amount on the surface of titanium disks, 3 uncoated disks per concentration were dip coated in 0, 1, 10, 25, 50, 100 and 250 mM of each IonL. The coatings were allowed to dry and then re-dissolved in 200 μL of ethanol by vortexing. Aliquots of the resulting ethanol-IonL solution were analyzed with ultraviolet-visible spectroscopy (UV-vis) at 340 nm for IonL-Phe and 250 nm for IonL-Met. A correlation was found between coating concentration and the re-dissolved aliquot concentration by using a calibration curve for both IonL-Phe and IonL-Met in ethanol at 0, 0.1, 0.25, 0.5, 1.0, 10, 25, 50, 100, and 250 mM. Final coating concentration was obtained from these data points using linear interpolation.

Coating morphology on different samples is shown in Figure 1. Immediately before surgery, coated and dried implants were placed under UV light for 1 hour to maintain sample sterility before implantation.

2.2 Animals

The twelve experimental groups consisted of three adult male 10 week old Lewis Rats (Charles River Laboratories, Wilmington, MA, USA) ranging from approximately 200 – 350 grams in weight. The rats were stored at the University of Texas at Dallas (Richardson, TX) vivarium throughout the study. Sterile water and dry food pellets were available to rats *ad libitum*, except for 72 hours following surgery, in which the diet was crumbled and mixed with water. Experimental groups of rats were separated by each dose and formulation of IonL (low, medium, high) as well as experimental time points (2 and 14 days after implantation) (n = 3 per group).

2.3 Surgical Procedure

Rats were weighed before and after surgery to monitor body weight. The animals were anaesthetized by an intramuscular injection of 50–100 mg/kg ketamine hydrochloride and 20–50 mg/kg xylazine hydrochloride. After anesthesia was administered rats were placed in a ventral decubitus position on a surgical table. A 4 × 5 cm area of the dorsal side of the rat was shaved and cleaned with povidone iodine in order to expose skin for implantation. A 1.5 cm incision was made down the sagittal plane of the rat's subcutaneous tissue approximately 7 cm from the base of the head and tail on either side, avoiding fascia or underlying muscle. After the incision was made, dissecting scissors were inserted under the skin on the left and right sides of the incision to resect the connective tissue away from the fascia, creating a pouch of approximately 4 × 2 cm on either side to place the implant. Each rat received 1 uncoated implant on the left side, and a coated implant on the right side. Sections of resected tissue without implants placed underneath the skin on the same rat were considered surgery shams and non-resected subcutaneous tissue adjacent to the implant site was considered control tissue during sample collection and analysis. After implantation, light pressure was

applied by the surgeon to the areas of resected tissue to help encourage wound closure. The incision was closed using 3 resorbable sutures. Following surgery, animals were given an injection at the surgical site with 20 mg/kg of lidocaine with 1:100,000 epinephrine (Quala Dental Products, Nashville, TN, USA) for local analgesia. At the end of the experimental periods (2 and 14 days), the animals were sacrificed with an overdose of pentobarbital sodium (Euthanasia III Med-Pharmex Inc., Pomona, CA, USA). After sacrifice, each tissue section containing an implant, as well as sham and control tissue was removed from the animal with dissecting scissors and placed in 10% neutral buffered formalin (NBF) for histology and molecular analysis. All surgeries, as well as pre-and post-operative care was carried out with supervision and approval from the Institutional Animal Care and Use Committee (IACUC #16–05).

2.4 Histological Processing

Fresh tissue samples were immediately collected after sacrifice and placed in 10% NBF for 48 hours for fixation. After fixation, they were continuously washed in water for 24 hours to prevent over fixing, and finally placed in 70% ethanol until processing. Before histological processing for paraffin embedding, samples were cut down to 10 mm² sections of tissue around the selected region of interest (ROI) of each sample type. Then, an incision was made into the capsule containing implants, and the implant was removed, leaving a small pocket. Tissue samples were bisected down the middle of the pocket and mounted in paraffin to achieve sections of the capsule at the same depth. Twelve 5 µm histological sections (technical replicates) from the central region of titanium implantation site were made per biological replicate: four sections at the surface of the embedded sample and eight sections 50 µm deeper into the tissue to capture variations in sections of the capsule. Twelve sections were made per sample to allow technical replicates of the capsule for histomorphometry. Two sections at each depth (four total) underwent a standard H&E stain for histomorphometry, selecting the best 3 technical replicates for counting. The remaining eight sections in each sample were used in technical duplicate for three markers and a negative control used for immunohistochemistry. Additionally, 10 µm ribbons of tissue after the last histological section were made and placed in Eppendorf tubes for molecular analysis.

2.5 Histopathological and Histomorphometric Analysis in H&E

Histopathological analysis was performed macroscopically to identify the presence of blood clots, blood vessels and inflammatory infiltrate (considering the percentage of different types of immune cells-polymorphonuclear cells (PMN), lymphocytes and macrophages), maturation of connective tissue (fibers and fibroblasts) and finally, the presence of foreign body giant cells (FBGC). Blood clot, blood vessels, fibroblasts and fibers density were also quantified using histomorphometry in order to determine possible differences among groups. From each sample, 3 technical replicates with the best view of the capsule (out of four) H&E sections were chosen for analysis comprising of seven 173.4 µm x 130.1 µm histological fields. These fields were located in the region adjacent to the Ti disc space and capsule surrounding it. Images were observed and captured using a 40x air objective (Olympus VS120, Shinjuku, Tokyo, Japan). A grid image was super imposed on each field, with 9 horizontal and 12 vertical lines creating and 108 points in a quadrangular area, using Image J software (Version 1.51, National Institutes of Health, Bethesda, MD, USA).

2.6 Immunohistochemistry

Immunohistochemistry was used to identify and quantify M0, M1 and M2 macrophages by using a universal macrophage marker (CD68, 1:100, Rabbit monoclonal [EPR20545], Abcam, Cambridge, UK), as well as M1 (CD86, 1:100, Mouse monoclonal [BU63], Abcam) and M2 markers (CD163, 1: 500, rabbit monoclonal [EPR19518], Abcam). Sections were first deparaffanized and underwent antigen retrieval by submersion in Tris Buffer pH= 9.0 maintained at 95 °C for 30 min. After washing with 0.05% PBST and Deionized (DI) water, the area of interest for staining was marked with a PAP pen. Tissue was blocked with 1% bovine serum albumin (1% BSA, in 1X phosphate buffered saline, Sigma-Aldrich, St. Louis, MO, USA) and subsequently incubated with the selected primary antibody at 4 °C overnight in a humidified chamber. A set of duplicate slides per sample were incubated with 1X PBS instead of a primary antibody as a negative control to confirm specific binding of secondary antibody. After incubation, the slides were washed and blocked with hydrogen peroxide, before incubation with a biotinylated goat anti-polyvalent secondary antibody and 3,3'-Diaminobenzidine (DAB) chromagen, following the manufacturer's protocol (mouse and rabbit specific HRP/DAB (ABC) and Micropolymer Detection IHC Kit, Abcam). Lastly slides were counterstained in Mayer's Hematoxylin for 2 minutes and finished with Permount™ (Fisher Scientific, Hampton, NH, USA) and a cover slip. In order to quantify the percentage of total macrophages expressing CD68, CD86 and CD163, 2 technical replicates from each marker were chosen and seven 173.4 µm x 130.1 µm histological fields were captured comprising the region adjacent to the Ti disc space. Cell counting was performed using the same technique employed with H&E stained sections.

2.7 Molecular Analysis

Ribbon samples from histological sectioning were used as tissue samples for gene expression analysis. After deparaffinization of samples with xylene, RNA of all samples was isolated using the RNeasy FFPE Mini-kit (Qiagen, Hilden Germany) following manufacturer's instructions. The concentration of the RNA was verified with a spectrophotometer (NanoDrop™ 200, Fisher Scientific, Hampton, NH, USA). After isolation, cDNA synthesis was performed using qScript cDNA Supermix (QuantaBio, Beverly, MA, USA), and cDNA reaction products were purified with the Qiaquick Purification Kit (Qiagen, Hilden Germany). qRT-PCR was performed with cDNA and TaqMan single tube assays (Applied Biosciences, Foster City, CA, USA) to quantify genes involved in macrophage polarization (ARG1, CD163), leukocyte and MSC recruitment (CCR5, CXCL12), as well as tissue regeneration/repair (VEGF-B, FGF1, Col1a2) using 15 ng/µL of cDNA per reaction. Each sample reaction was performed in duplicate and contained a gDNA and reverse transcription control to confirm that there was only template specific amplification. Data analysis was performed using the Ct method to compare each marker of interest with 2 housekeeping genes (B2m, Hprt), determining fold changes in uncoated Ti and IonL coated Ti relative to a non-surgery control.

2.8 Statistical Analysis

Statistical analysis of histomorphometry in H&E and IHC was performed using a two-way Analysis of Variance with a post hoc Tukey test considering time and dose within IonL-Phe

or IonL-Met as factors. The Tukey test made multiple comparisons to evaluate the significance between the factors. qPCR statistical analysis was performed using a one way analysis of variance to compare dose within both formulations. Both tests were run in GraphPad Prism 5.0 software (GraphPad Software Inc., San Diego, CA, USA) using a significance level (α) of 0.05. Statistical significance of comparisons between different data sets was determined using the p-value.

3. Results

3.1 Coating Morphology

Coating morphology was visualized through SEM to analyze topographical characteristics of the different doses and formulations of IonL on titanium disks prior to implantation. IonL-Phe exhibited small, sparse droplets at the low dose, while quickly exhibiting self-aggregating behavior at medium and high doses that was not uniform over the disk surface, as shown in Figure 2. On the contrary, IonL-Met resulted in slightly larger uniform droplets across the surface at the low dose and medium dose. At high doses there was observed self-aggregating and crystallization behavior, forming larger droplets that were evenly spaced on the surface.

3.2 Clinical, Histopathological and Histomorphometric Analysis

From a clinical perspective, rats exhibited no signs of hyperalgesia, with normal grooming, eating and nesting behavior. No incisions or implantation sites exhibited signs of infection, excessive swelling and redness 24 hours following surgery. Upon sacrifice and sample collection, macroscopic evaluation evidenced that uncoated samples were encapsulated by a thin membrane in all samples at 2 and 14 days. Microscopically, uncoated samples at 2 days stained with H&E were surrounded by a residual blood clot which provided an initial provisional matrix formed by fibrin network and permeated with inflammatory infiltrate containing PMN and mononuclear leukocytes, shown in Figure 3. At 14 days, there was a thin organized fibroblast-rich connective tissue surrounding Ti disks with visually reduced inflammatory infiltrate and no foreign body giant cells (FBGC) at the site of implantation. Histomorphometric analysis in Figure 4. supports visual observations regarding soft tissue health at 2 and 14 days. Blood clot area is reduced in most samples from 2 to 14 days, while blood vessel density and connective tissue (fibers+fibroblasts) is unchanged over time

Coated samples stained with H&E demonstrated the same sequence of inflammatory response and healing outcome from 2 to 14 days as uncoated Ti (Figure 3). However there were some observable differences between coated and uncoated samples. At 2 days, coated samples with medium and high doses exhibited an amorphous material lining the space left by the surface of Ti disks, in contact with the surrounding connective tissue. On the other hand, low doses of both formulations of IonL and uncoated Ti did not exhibit this structure. At 14 days, there was no indication of this evident IonL coating residue, and all coated presented a notable decrease of inflammatory infiltrate (PMN and lymphocytes), with varying amounts of macrophages and fibroblasts within the newly formed connective tissue surrounding the Ti space. It was also noted that high dose IonL-Phe appeared macroscopically to have elevated amounts of inflammatory infiltrate when compared to

other samples at this time point. All doses of IonL-Met samples, and low/medium doses of IonL-Phe showed a thinner and more organized fibroblast-rich connective tissue surrounding Ti disks, as observed with uncoated Ti, when compared to high dose IonL-Phe. The high dose IonL-Phe capsule appears thicker and more fibrous with negligible quantities of fibroblasts. Importantly, no FBGC were observed in the sites of implantation of coated samples, even when high doses of IonL were used. Histomorphometrically, blood clot varied in all all coated at 2 days, but was reduced at 14 days in all samples, except for medium dose IonL-Phe. Blood vessels exhibited similar area density at 2 days and at 14 days, most coated samples had similar levels or an increase from their 2 day vessel density, however high dose IonL-Phe had a decreasing density trend. Levels of fibers + fibroblasts were not significantly different at 2 and 14 days amongst experimental groups.

3.3 Immunohistochemistry for Macrophages

Immunohistochemistry was performed in order to confirm and quantify the presence of macrophages, as well their M1 and M2 subtypes. Thus, CD68 was used as universal macrophage marker, CD86 was used as an M1 marker and CD163 as an M2 marker. Visual observation indicated all three macrophage types were present in uncoated controls at 2 days as shown in Figure 5. The proportions of each marker were similar at both 2 and 14 days, with CD68+ and CD163+ cells being the most populous, followed by CD86+. At 2 days all macrophages were seen adjacent to the connective tissue capsule. At 14 days, CD163+ cells were seen mostly adjacent to the connective tissue capsule surrounding the uncoated Ti disks, while CD68+ and CD86+ positive cells were seen lining the implant-tissue interface. The quantity of CD68+ and CD163 + macrophages in uncoated samples were similar at 2 and 14 days, while there was a slight increase of CD86+ macrophages at 14 days compared to 2 days. Ionic liquid coated samples exhibited the same pattern of residence at 2 and 14 days, but also exhibited clusters of macrophages (identified by size and morphology) residing in the capsule itself at 14 days. However, these capsule macrophages did not stain positive for any of the three markers.

When the different IonL formulations were compared to the uncoated control, as shown in Figure 6, it was revealed that CD68+ cells in low dose IonL-Phe samples were significantly higher than uncoated samples, low and high dose of IonL-Met, and medium dose of IonL-Phe implants ($p < 0.05$). At 14 days, CD68+ density of all samples were reduced to quantities similar to the uncoated Ti, although there was a trend that suggested that as the IonL dose increased, so did the CD68+ density. Similar behavior regarding low dose IonL-Phe was observed in CD86+ cells, which had significantly higher quantities than uncoated Ti, but was not significantly different than all other coated samples. At 14 days, CD86+ density all for coated samples was not significantly different to each other or the uncoated Ti, with only the medium dose IonL-Met showing a non-significant increase in expression. CD163+ density was not significantly different than the uncoated samples, but again had similar trends to the CD68 marker at 14 days, showing elevated density as the dosage increased. Overall, IonL-Met coated samples showed non-significant differences of macrophage area density at 2 days compared to uncoated controls, while IonL-Phe had significantly higher density in all doses. This behavior was also observed at 14 days, but with a trend that

showed an increase in density corresponding to an increased dose amount in both formulations.

3.4 qPCR

qPCR was performed to supplement histomorphometry and immunohistochemistry results, allowing the analysis of 7 markers representative of chemotaxis of immune cells, macrophage polarization, MSC recruitment, angiogenesis and capsule development processes. At 2 days Uncoated samples exhibited an up regulation of markers for chemotaxis of immune cells (CCR5, CD163, CXCL12) as well as an up regulation in markers for angiogenesis (VEGFA) and fibroblast/connective tissue growth (FGF1, COL1A2) compared to the non-surgery control. At 14 days, CCR5, CD163, and VEGFA had down regulated from 2 days while M2 Marker ARG-1, CXCL12 (also a marker for MSC recruitment), FGF1, and COL1A2 had higher fold changes than the uncoated sample at 2 days. Considering the response of the IonL-coated samples to the uncoated samples, chemotaxis of immune cells and macrophages (CCR5, ARG-1, CD163, CXCL12) were elevated to similar or higher levels than uncoated Ti in both coatings at all doses, seen in Figure 7. At 14 days, CCR5, a chemokine receptor involved in macrophage migration, was down regulated to a fold change similar to the uncoated control in low and medium doses, while high doses still had a higher fold change than uncoated samples at this time point. At 2 days markers for angiogenesis and connective tissue/fibroblast growth (COL1A2, FGF1, VEGFA) were similar to the uncoated Ti, except for high dose IonL-Met, which showed a non-significant increase in FGF1. At 14 days, all coated samples showed up-regulation of CXCL12 similar to uncoated Ti. However, low and medium doses of both coatings exhibited the elevated levels of FGF1, COL1A2 at 14 days, similar to uncoated Ti, while FGF1 at the high doses showed a non-significant decrease in fold change compared to uncoated Ti. VEGFA expression levels remained relatively stable across all time points, regardless of coating formulation or dose.

4. Discussion

Current approaches in the field of titanium based implants seek to prevent implant related complications through various types of surface modifications.^{29,30,42,43} IonLs have recently been proposed as a potential multifunctional coating approach for titanium, providing corrosion resistance, lubrication and selective toxicity towards bacteria composing oral biofilms while maintaining host cell compatibility *in vitro*.^{37–39} However, it is important to consider that *in vivo* host/biomaterial interface is substantially more complex than simulated conditions *in vitro*. Following the initial trauma of placement there is release of numerous pro- and anti-inflammatory molecules and growth factors, which ultimately influence the recruitment of different cell subtypes and polarization of macrophages.^{44–47} Therefore, the goal of this work was to test the effect of IonL-Phe and IonL-Met on the events following the early healing period, which currently represent a new generation of coatings for titanium implants. The events following the early healing period are critical for biomaterial integration, and this work has demonstrated a new coating modality does not interfere with this healing timeline. It was hypothesized that low and medium doses of both formulations

would likely maintain the normal healing progression necessary for tissue regeneration without effecting the FBR of titanium.

Subcutaneous model implantation has been classically used in rodents for testing the host response of different biomaterials, such as titanium^{44,48,49}, various tissue scaffolds made from animal or plant based molecules^{50,51}, and synthetic hydrogels or polymers.⁵² In general, the host response observed with this model, first involves acute inflammation associated with the injury of placement, identified by presence of polymorphonuclear cells (PMN), mononuclear cells (MN), and blood clots. In the later stages of this response, PMN and MN populations decrease, giving way to a densely packed connective tissue surrounding the implant, populated fibroblasts and new blood vessels, as observed in Figure 3.¹⁶ At this stage, FBGCs are often found in implantations with hydrogel or polymer based materials, attempting to resorb the implanted biomaterials.^{16,50,53,54} However, titanium implantation has been shown to exhibit only a small degree of inflammation 72 hours post implantation and complete healing and resolution around 14 days without the presence of FBGC in subcutaneous tissue in C57Bl/6 mice.⁴⁴ Accordingly, our results demonstrated that the early healing progression of uncoated Ti, shown in Figure 3, demonstrated similar histological and histomorphometric features to those described in previous studies using uncoated Ti, despite using a rat model rather than a murine model. This observation corroborates the suitability of this model for the first *in vivo* characterization of IonL coatings.

Although certain surface treatments performed on titanium can help address failure modes, it has been shown that these treatments induce potential effects on the FBR to an implant.^{16,55–57} *In vitro*, the IonL coating demonstrated stable coating on Ti able to release from the surface after 7 days in solution.³⁹ In the *in vivo* subcutaneous model, only samples from 2 day time point containing medium and high doses of both IonL formulations presented residual quantities of IonL coatings, identified as an amorphous structure delineating the space previously occupied by the coating on the implant surface (Figure 3, indicated by arrows). However, this structure was no longer observed at 14 days, suggesting that this structure was the IonL eluting into surrounding tissues and/or resorbed by macrophages, corroborating this *in vitro* behavior. Also important, no FBGC were observed in sites of coated samples, resembling the response observed in uncoated Ti. The absence of FBGC cells at both time points, along with the proposed elution behavior of the coating, suggest that the IonL was biodegradable under these conditions and does not elicit a strong FBR, even in high doses. This elution behavior is in agreement with previous results *in vitro*, where approximately 40% and 80% of IonL-Phe and IonL-Met on a Ti disk had released into PBS after 7 days of immersion, respectively.³⁹

As a result of the injury caused by implant placement, a cascade of inflammatory events begin with the release of pro-inflammatory molecules, which includes the induction or upregulation of chemokines²⁰, which mediate the recruitment of different cell subsets into the chemotactic gradients via specific chemokine receptors. For example, CXCL12 recruits mesenchymal stem cell (MSC) homing into wound healing sites via CXCR4 receptor^{58,59}, while chemokine receptor CCR5 mediate inflammatory monocytes/macrophages traffic into injured tissues in response to chemokines such as CCL5.^{60,61} Additionally, as the implant healing evolves in the subcutaneous tissue, expression of different growth factors (e.g. FGF,

VEGF) and matrix markers (Col1a2) significantly increase.⁴⁴ In addition to macrophage chemoattraction, its polarization at response sites into pro-inflammatory (M1) or anti-inflammatory (M2) phenotypes can ultimately decide the fate of regeneration around an implant.⁴⁷ It has been previously demonstrated in a subcutaneous implantation model in C57Bl/6 mice that titanium (Ti) exhibited a low intensity inflammatory response, with expression of both M1 markers (CD86) and M2 markers (CD163, ARG-1) present during acute inflammation, with M2 macrophages dominating towards the resolution of chronic inflammation.^{20,44} Importantly, the behavior observed for control implants in the current model are in accordance with the observations from these previous studies. Indeed, uncoated Ti samples exhibited up-regulation of CCR5, CXCL12 and CD163 at 2 days (Figure 7), along with representation from all macrophage subtypes (CD68, CD86, and CD163, Figure 5 and 6) indicating the recruitment of PMN and MN cells to the injury site. Additionally, at 14 days, CXCL12 and FGF1 was up-regulated from the 2-day time point, indicating MSC recruitment and connective tissue development, in accordance with the literature.^{58,59,62} This trend was also observed with both molecular markers for M2 polarization (ARG-1, CD163) and quantities of CD163 macrophages increased at this time-point, corroborating this observation.

Moreover, it is important to consider how the IonL can impact this inflammatory cascade. Interestingly, in all the IonL-coated group there was an increasing trend in the presence of M1 and M2 macrophages according to IHC in addition to the upregulation of chemotactic and macrophage markers (CCR5, CD163, ARG-1) in comparison with uncoated control at 2 days. Also, this elevation was significant for both CD68 and CD163 markers in low dose IonL-Phe. Importantly, while the macrophages presence was increased, the overall M1/M2 ratio/balance associated with a favorable healing outcome in the control (uncoated) group seems to be preserved.

Although assessing acute inflammation is important, the 14-day time point is a better indicator of the effects of IonL on the resolution of inflammation and healing outcome, indicating whether or not the coating is affecting the successful interaction and incorporation of the biomaterial by host connective tissue.^{17,44} Histopathologically, inflammatory resolution in low and medium doses of both IonL coatings was similar to uncoated controls: clearing of blood clot, formation of new vessels, capsules with well-developed connective tissue containing fibroblasts (Figure 3).⁴⁴ However, there were some subtle differences in relation to the low and medium dose IonL formulations, and some significant differences in the high dose IonL in capsule composition. In coated samples there was resolution of elevated acute inflammation supported by qPCR results (down regulation of CCR5 CD163) and IHC markers. However, visually the capsule was populated with macrophages in addition to fibroblasts in low and medium doses in both compositions. There was a similar expression of MSC recruitment marker CXCL12 in comparison to the control as well as other angiogenesis and tissue growth markers (VEGFA, FGF1, and COL1A2) at this time point. In high doses, the fibroblast presence trended lower in both formulations as evidenced by a down regulation of FGF1 markers compared to the uncoated control at 14 days (Figure 7). Interestingly, similar behavior has been observed *in vitro* with fibroblasts in the presence of IonLs of this concentration.³³ The higher doses of these IonLs were intentionally selected above the IC₅₀ of fibroblasts *in vitro*. So potentially detrimental responses such as the

downregulation of FGF1 were anticipated and are supported by the known cytotoxicity of this IonL dose. Regardless, histomorphometry indicated overall connective tissue health similar to the uncoated control. Macrophages indicated a trend where there was an elevation of inflammatory cells that is increasing proportionally in IonL-Met doses, although additional studies will be needed to confirm this trend. Evidence suggests that ideally during resolution of inflammation a larger proportion of M2 macrophages is desired to achieve successful integration, although there is no consensus on the ideal M1/M2 ratio.¹⁷ Additionally, there was also an interesting behavior observed with location of M1 and M2 macrophages at 14 days, with the majority of the uncoated Ti samples having M2 macrophages outside of the capsule, with a small amount of M1 populating the lining (Figure 5). This was also true of coated samples, although there was more evidence of M1 macrophages in the lining of the biomaterial/tissue interface. The literature has observed this spatiotemporal behavior of macrophages, specifying that there can be populations of a particular phenotype based on local microenvironments.⁶³ M1 macrophages are often observed at the biomaterial/tissue interface, and it has been suggested that observing both M1 and M2 markers in this location will actually prolong the FBR, whereas having M2 populations not immediately adjacent to the implant surface is implicating in reducing the FBR, as observed in this study.^{17,63}

Regardless of the phenotypes of macrophages present in all samples, the results suggest that even at high IonL doses regeneration of host tissue can likely be achieved, although medium doses of both formulations have the response most similar to uncoated Ti samples. When considering if one formulation is more suitable for this application, IonL-Phe exhibits a less consistent droplet morphology and immune response amongst different doses compared to IonL-Met. These behaviors can be attributed to the more hydrophobic nature of IonL-Phe, which is worth nothing as hydrophobic surface modifications to Ti are associated with up-regulation of pro-inflammatory cytokines.⁶⁴ On the other hand, the more hydrophilic IonL-Met produces a consistently uniform coating at low and medium doses, while also maintaining Ti biocompatibility. As this is the first *in vivo* biocompatibility study performed on IonL coatings, some limitations of the model need to be discussed. This model involved an implantation into subcutaneous tissue in rats, which is useful for evaluating the inflammatory response to a novel material, allowing a large area of contact between the biomaterial and host tissue in the absence of complicating oral factors compared to the osseointegration models used in rats and mice.^{16,44} While this model does not simulate the biological environment that most Ti implants are expected to perform in, the overall inflammatory immune response which would in theory impact osseointegration was described to be remarkably similar in osseous and subcutaneous compartments.⁴⁴ However, despite the strong indications towards maintenance of Ti biocompatibility, the current model does not allow a definitive statements regarding the extent that these coatings can impact osseointegration, and also the efficacy in which the coating can prevent conditions which challenge osseointegration. In particular, dental implants are subjected to the presence of oral microbiota, saliva, different compositions of bone and oral mucosa which cannot be simulated in a subcutaneous environment.²⁰ Future studies will use the best performing IonL in a more relevant oral rodent osseointegration model in order to assess not only its efficacy as a multifunctional coating, but also its overall impact on early stage of Ti osseointegration.

This new generation of coatings have the potential to improve chances for clinical success by maintaining the biocompatibility of Ti implants, while demonstrating properties that can prevent the chance of implant complications.

5. Conclusion

Taking in consideration all metrics, both IonL formulations induced a slightly increased acute inflammatory response that was resolved most similarly to uncoated Ti in medium doses that does not significantly affect early healing overall. Due to the uniformity of the coating produced by IonL-Met, this formulation might be preferable for a consistent host response. This study demonstrated that IonL at the appropriate concentration confers coating morphology and release behavior on titanium without significantly interfering with healing and Ti foreign body response.

Acknowledgements:

The authors would like to thank Jacob D. Wade and Jordan Chen for assisting with histomorphometry measurements. We would also like to thank John M. Shelton, Diana Wigginton, Cameron Perry, and Jessica Williams from the University of Texas Southwestern Medical Center Histo Pathology core for their guidance, expertise and services. Finally, we would like to thank Dr. Zachary Campbell, Dr. Tae Hoon Kim and Tzu-Fang Lou for allowing us to use their equipment for qPCR analysis. This study was supported by a grant by the National Institute of Dental and Craniofacial Research (NIDCR/NIH) (Project #1R01DE026736-01A1).

References

- (1). Niinomi M. Mechanical biocompatibilities of titanium alloys for biomedical applications. *J. Mech. Behav. Biomed. Mater* 2008, 1 (1), 30–42 DOI: 10.1016/j.jmbbm.2007.07.001. [PubMed: 19627769]
- (2). T A; C J. Osteoinduction, osteoconduction and osseointegration. *Eur. Spine J* 2001, 10 (Supplement 2), S96–S101 DOI: 10.1007/s005860100282. [PubMed: 11716023]
- (3). Manor Y; Oubaid S; Mardinger O. Characteristics of Early Versus Late Implant Failure : A Retrospective Study. *YJOMS* 2009, 67 (12), 2649–2652 DOI: 10.1016/j.joms.2009.07.050.
- (4). Norowski PA; Bumgardner JD Biomaterial and antibiotic strategies for peri-implantitis: A review. *J. Biomed. Mater. Res. Part B Appl. Biomater* 2009, 88B (2), 530–543 DOI: 10.1002/jbm.b.31152.
- (5). Snauwaert K; Duyck J; van Steenberghe D; Quirynen M; Naert I. Time dependent failure rate and marginal bone loss of implant supported prostheses: a 15-year follow-up study. *Clin. Oral Investig* 2000, 4 (1), 0013–0020 DOI: 10.1007/s007840050107.
- (6). Moraschini V; Poubel LADC; Ferreira VF; Barboza EDSP Evaluation of survival and success rates of dental implants reported in longitudinal studies with a follow-up period of at least 10 years: A systematic review. *Int. J. Oral Maxillofac. Surg* 2015, 44 (3), 377–388 DOI: 10.1016/j.ijom.2014.10.023. [PubMed: 25467739]
- (7). Wittneben J; Buser D; Salvi GE; Bürgin W; Hicklin S; Brägger U. Complication and Failure Rates with Implant-Supported Fixed Dental Prostheses and Single Crowns: A 10-Year Retrospective Study. *Clin. Implant Dent. Relat. Res* 2014, 16 (3), 356–364 DOI: 10.1111/cid.12066. [PubMed: 23551688]
- (8). Becker W; Hujoel P; Becker BE; Wohrle P. Dental Implants in an Aged Population: Evaluation of Periodontal Health, Bone Loss, Implant Survival, and Quality of Life. *Clin. Implant Dent. Relat. Res* 2016, 18 (3), 473–479 DOI: 10.1111/cid.12340. [PubMed: 26082299]
- (9). Sridhar S; Wang F; Wilson TG; Valderrama P; Palmer K; Rodrigues DC Multifaceted roles of environmental factors toward dental implant performance: Observations from clinical retrievals and in vitro testing. *Dent. Mater* 2018, 34 (11), e265–e279 DOI: 10.1016/j.dental.2018.08.299. [PubMed: 30220507]

- (10). Renvert S; Polyzois I; Maguire R. Re-osseointegration on previously contaminated surfaces: A systematic review. *Clin. Oral Implants Res* 2009, 20 (SUPPL. 4), 216–227 DOI: 10.1111/j.1600-0501.2009.01786.x. [PubMed: 19663967]
- (11). Subramani K; Wismeijer D. Decontamination of titanium implant surface and re-osseointegration to treat peri-implantitis: a literature review. *The International journal of oral & maxillofacial implants*. 2012, pp 1043–1054. [PubMed: 23057016]
- (12). Koldslund OC; Scheie AA; Aass AM Prevalence of Implant Loss and the Influence of Associated Factors. *J. Periodontol* 2009, 80 (7), 1069–1075 DOI: 10.1902/jop.2009.080594. [PubMed: 19563286]
- (13). Malm MO; Jemt T; Stenport V. Early Implant Failures in Edentulous Patients: A Multivariable Regression Analysis of 4615 Consecutively Treated Jaws. A Retrospective Study. *J. Prosthodont* 2018, 27 (9), 803–812 DOI: 10.1111/jopr.12985. [PubMed: 30307086]
- (14). Esposito M; Thomsen P; Ericson LE; Lekholm U. Histopathologic observations on early oral implant failures. *Int. J. Oral Maxillofac. Implants* 2000, 14 (6), 798–810.
- (15). Santos MCLG; Campos MIG; Line SRP Early dental implant failure : A review of the literature. *Brazilian J. Oral Sci* 2002, 1 (3), 103–111.
- (16). Kastellorizios M; Tipnis N; Burgess DJ Foreign Body Reaction to Subcutaneous Implants. In *Advances in Experimental Medicine and Biology*; 2015; pp 93–108.
- (17). Corradetti B. *The Immune Response to Implanted Materials and Devices*; Corradetti B, Ed.; Springer International Publishing: Cham, 2017.
- (18). Trindade R; Albrektsson T; Tengvall P; Wennerberg A. Foreign Body Reaction to Biomaterials: On Mechanisms for Buildup and Breakdown of Osseointegration. *Clin. Implant Dent. Relat. Res* 2016, 18 (1), 192–203 DOI: 10.1111/cid.12274. [PubMed: 25257971]
- (19). Thalji GN; Nares S; Cooper LF Early molecular assessment of osseointegration in humans. *Clin. Oral Implants Res* 2014, 25 (11), 1273–1285 DOI: 10.1111/clr.12266. [PubMed: 24118318]
- (20). Bigueti CC; Cavalla F; Silveira EM; Fonseca AC; Vieira AE; Tabanez AP; Rodrigues DC; Trombone APF; Garlet GP Oral implant osseointegration model in C57Bl/6 mice: microtomographic, histological, histomorphometric and molecular characterization. *J. Appl. Oral Sci* 2018, 26 DOI: 10.1590/1678-7757-2017-0601.
- (21). Trindade R; Albrektsson T; Wennerberg A. Current Concepts for the Biological Basis of Dental Implants: Foreign Body Equilibrium and Osseointegration Dynamics. *Oral Maxillofac. Surg. Clin. North Am* 2015, 27 (2), 175–183 DOI: 10.1016/j.coms.2015.01.004. [PubMed: 25753575]
- (22). Marfo KA; Berend KR; Morris MJ; Adams JB; Lombardi AV Mid-Term Results of Modular Tapered Femoral Stems in Revision Total Hip Arthroplasty. *Surg. Technol. Int* 2019, 35. [PubMed: 30825320]
- (23). Wirries N; Winneken HJ; Lewinski G. von; Windhagen H; Skutek M. Osteointegrative Sleeves for Metaphyseal Defect Augmentation in Revision Total Knee Arthroplasty: Clinical and Radiological 5-Year Follow-Up. *J. Arthroplasty* 2019 DOI: 10.1016/j.arth.2019.04.024.
- (24). Trindade R; Albrektsson T; Tengvall P; Wennerberg A. Foreign Body Reaction to Biomaterials: On Mechanisms for Buildup and Breakdown of Osseointegration. *Clin. Implant Dent. Relat. Res* 2016, 18 (1), 192–203 DOI: 10.1111/cid.12274. [PubMed: 25257971]
- (25). Rodrigues DC; Valderrama P; Wilson TG; Palmer K; Thomas A; Sridhar S; Adapalli A; Burbano M; Wadhvani C. Titanium corrosion mechanisms in the oral environment: A retrieval study. *Materials (Basel)*. 2013, 6 (11), 5258–5274 DOI: 10.3390/ma6115258. [PubMed: 28788388]
- (26). Rodrigues DC; Urban RM; Jacobs JJ; Gilbert JL In vivo severe corrosion and hydrogen embrittlement of retrieved modular body titanium alloy hip-implants. *J. Biomed. Mater. Res. - Part B Appl. Biomater* 2009, 88 (1), 206–219 DOI: 10.1002/jbm.b.31171. [PubMed: 18683224]
- (27). Albrektsson T; Dahlin C; Jemt T; Sennerby L; Turri A; Wennerberg A. Is Marginal Bone Loss around Oral Implants the Result of a Provoked Foreign Body Reaction? *Clin. Implant Dent. Relat. Res* 2014, 16 (2), 155–165 DOI: 10.1111/cid.12142. [PubMed: 24004092]
- (28). Mouhyi J; Dohan Ehrenfest DM; Albrektsson T. The Peri-Implantitis: Implant Surfaces, Microstructure, and Physicochemical Aspects. *Clin. Implant Dent. Relat. Res* 2012, 14 (2), 170–183 DOI: 10.1111/j.1708-8208.2009.00244.x. [PubMed: 19843108]

- (29). Liu R; Tang Y; Zeng L; Zhao Y; Ma Z; Sun Z; Xiang L; Ren L; Yang K. In vitro and in vivo studies of anti-bacterial copper-bearing titanium alloy for dental application. *Dent. Mater* 2018, 34 (8), 1112–1126 DOI: 10.1016/j.dental.2018.04.007. [PubMed: 29709241]
- (30). Besinis A; Hadi SD; Le HR; Tredwin C; Handy RD Antibacterial activity and biofilm inhibition by surface modified titanium alloy medical implants following application of silver, titanium dioxide and hydroxyapatite nanocoatings. *Nanotoxicology* 2017, 11 (3), 327–338 DOI: 10.1080/17435390.2017.1299890. [PubMed: 28281851]
- (31). Le Guéhennec L; Soueidan A; Layrolle P; Amouriq Y. Surface treatments of titanium dental implants for rapid osseointegration. *Dent. Mater* 2007, 23 (7), 844–854 DOI: 10.1016/j.dental.2006.06.025. [PubMed: 16904738]
- (32). Wennerberg A; Albrektsson T. On implant surfaces: a review of current knowledge and opinions. *Int. J. Oral Maxillofac. Implants* 2009, 25 (1), 63–74 DOI: 10.1111/j.1600-051X.2008.01321.x.
- (33). Gindri IM; Siddiqui DA; Bhardwaj P; Rodriguez LC; Palmer KL; Frizzo CP; Martins MAP; Rodrigues DC Dicationic imidazolium-based ionic liquids: a new strategy for non-toxic and antimicrobial materials. *RSC Adv.* 2014, 4 (107), 62594–62602 DOI: 10.1039/C4RA09906K.
- (34). Zhou F; Liang Y; Liu W. Ionic liquid lubricants: designed chemistry for engineering applications. *Chem. Soc. Rev* 2009, 38 (9), 2590–2599 DOI: 10.1039/b817899m. [PubMed: 19690739]
- (35). Marrucho IM; Branco LC; Rebelo LPN Ionic Liquids in Pharmaceutical Applications. *Annu. Rev. Chem. Biomol. Eng* 2014, 5 (1), 527–546 DOI: 10.1146/annurev-chembioeng-060713-040024. [PubMed: 24910920]
- (36). Johnson KE What's an Ionic Liquid? *Electrochem. Society Interface* 2007, 16 (1), 38–41.
- (37). Gindri IM; Siddiqui DA; Frizzo CP; Martins MAPP; Rodrigues DC; Rodrigues C; Rodrigues DC Ionic Liquid Coatings for Titanium Surfaces: Effect of IL Structure on Coating Profile. *ACS Appl. Mater. Interfaces* 2015, 7 (49), 27421–27431 DOI: 10.1021/acsami.5b09309.
- (38). Gindri IM; Siddiqui DA; Frizzo CP; Martins MAP; Rodrigues DC; Davis C; Frizzo CP; Martins MAP; Rodrigues DC Improvement of tribological and anti-corrosive performance of titanium surfaces coated with dicationic imidazolium-based ionic liquids. *RSC Adv.* 2016, 6 (82), 78795–78802 DOI: 10.1039/C6RA13961B.
- (39). Gindri IM; Palmer KL; Siddiqui DA; Aghyarian S; Frizzo CP; Martins MAP; Rodrigues DC Evaluation of Mammalian and Bacterial Cell Activity on Titanium Surface Coated with Dicationic Imidazolium-based Ionic Liquids. *RSC Adv.* 2016, 6 (43), 36475–36483 DOI: 10.1039/C6RA01003B.
- (40). Gindri IM; Frizzo CP; Bender CR; Tier AZ; Martins M. a P.; Villetti M.a; Machado G; Rodriguez LC; Rodrigues DC Preparation of TiO₂ Nanoparticles Coated with Ionic Liquids: A Supramolecular Approach. *ACS Appl. Mater. Interfaces* 2014, 6 (14), 11536–11543 DOI: 10.1021/am5022107. [PubMed: 24933673]
- (41). Fukumoto K; Yoshizawa M; Ohno H. Room Temperature Ionic Liquids from 20 Natural Amino Acids. *J. Am. Chem. Soc* 2005, 127 (8), 2398–2399 DOI: 10.1021/ja043451i. [PubMed: 15724987]
- (42). Visai L; de Nardo L; Punta C; Melone L; Cigada A; Imbriani M; Arciola CR Titanium oxide antibacterial surfaces in biomedical devices. *Int. J. Artif. Organs* 2011, 34 (9), 929–946 DOI: 10.5301/ijao.5000050. [PubMed: 22094576]
- (43). Gaviria L; Salcido JP; Guda T; Ong JL Current trends in dental implants. *J. Korean Assoc. Oral Maxillofac. Surg* 2014, 40 (2), 50–60 DOI: 10.5125/jkaoms.2014.40.2.50. [PubMed: 24868501]
- (44). Biguetti CC; Cavalla F; Silveira EV; Tabanez AP; Francisconi CF; Taga R; Campanelli AP; Trombone APF; Rodrigues DC; Garlet GP HGMB1 and RAGE as Essential Components of Ti Osseointegration Process in Mice. *Front. Immunol* 2019, 10 DOI: 10.3389/fimmu.2019.00709.
- (45). Christo SN; Diener KR; Bachhuka A; Vasilev K; Hayball JD Innate Immunity and Biomaterials at the Nexus: Friends or Foes. *Biomed Res. Int* 2015, 2015, 1–23 DOI: 10.1155/2015/342304.
- (46). Anderson JM; Rodriguez A; Chang DT Foreign body reaction to biomaterials. *Semin. Immunol* 2008, 20 (2), 86–100 DOI: 10.1016/j.smim.2007.11.004. [PubMed: 18162407]
- (47). Brown BN; Ratner BD; Goodman SB; Amar S; Badylak SF Macrophage polarization: An opportunity for improved outcomes in biomaterials and regenerative medicine. *Biomaterials* 2012, 33 (15), 3792–3802 DOI: 10.1016/j.biomaterials.2012.02.034. [PubMed: 22386919]

- (48). Matsuno H. Biocompatibility and osteogenesis of refractory metal implants, titanium, hafnium, niobium, tantalum and rhenium. *Biomaterials* 2001, 22 (11), 1253–1262 DOI: 10.1016/S0142-9612(00)00275-1. [PubMed: 11336297]
- (49). Tîlmaciu CM; Mathieu M; Lavigne JP; Toupet K; Guerrero G; Ponche A; Amalric J; Noël D; Mutin PH In vitro and in vivo characterization of antibacterial activity and biocompatibility: A study on silver-containing phosphonate monolayers on titanium. *Acta Biomater.* 2015, 15, 266–277 DOI: 10.1016/j.actbio.2014.12.020. [PubMed: 25562573]
- (50). Modulevsky DJ; Cuerrier CM; Pelling AE Biocompatibility of Subcutaneously Implanted Plant-Derived Cellulose Biomaterials. *PLoS One* 2016, 11 (6), e0157894 DOI: 10.1371/journal.pone.0157894.
- (51). Lucke S; Hoene A; Walschus U; Kob A; Pissarek J-W; Schlosser M. Acute and Chronic Local Inflammatory Reaction after Implantation of Different Extracellular Porcine Dermis Collagen Matrices in Rats. *Biomed Res. Int* 2015, 2015, 1–10 DOI: 10.1155/2015/938059.
- (52). Gu B; Papadimitrakopoulos F; Burgess DJ PLGA microsphere/PVA hydrogel coatings suppress the foreign body reaction for 6 months. *J. Control. Release* 2018, 289, 35–43 DOI: 10.1016/j.jconrel.2018.09.021. [PubMed: 30261203]
- (53). Kao WJ; McNally AK; Hiltner A; Anderson JM Role for interleukin-4 in foreign-body giant cell formation on a poly(etherurethane urea) in vivo. *J. Biomed. Mater. Res* 1995, 29 (10), 1267–1275 DOI: 10.1002/jbm.820291014. [PubMed: 8557729]
- (54). Christenson EM; Dadsetan M; Anderson JM; Hiltner A. Biostability and macrophage-mediated foreign body reaction of silicone-modified polyurethanes. *J. Biomed. Mater. Res. Part A* 2005, 74A (2), 141–155 DOI: 10.1002/jbm.a.30317.
- (55). Alfarsi MA; Hamlet SM; Ivanovski S. Titanium surface hydrophilicity modulates the human macrophage inflammatory cytokine response. *J. Biomed. Mater. Res. -Part A* 2014, 102 (1), 60–67 DOI: 10.1002/jbm.a.34666.
- (56). Lee RSB; Hamlet SM; Ivanovski S. The influence of titanium surface characteristics on macrophage phenotype polarization during osseous healing in type I diabetic rats: a pilot study. *Clin. Oral Implants Res* 2017, 28 (10), e159–e168 DOI: 10.1111/clr.12979. [PubMed: 27637574]
- (57). Scisłowska-Czarnecka A; Menaszek E; Szaraniec B; Kolaczowska E. Ceramic modifications of porous titanium: Effects on macrophage activation. *Tissue Cell* 2012, 44 (6), 391–400 DOI: 10.1016/j.tice.2012.08.002. [PubMed: 22939219]
- (58). Hocking AM The Role of Chemokines in Mesenchymal Stem Cell Homing to Wounds. *Adv. Wound Care* 2015, 4 (11), 623–630 DOI: 10.1089/wound.2014.0579.
- (59). Yellowley C. CXCL12/CXCR4 signaling and other recruitment and homing pathways in fracture repair. *Bonekey Rep.* 2013, 2 (3) DOI: 10.1038/bonekey.2013.34.
- (60). Bigueti CC; Vieira AE; Cavalla F; Fonseca AC; Colavite PM; Silva RM; Trombone APF; Garlet GP CCR2 Contributes to F4/80+ Cells Migration Along Intramembranous Bone Healing in Maxilla, but Its Deficiency Does Not Critically Affect the Healing Outcome. *Front. Immunol* 2018, 9 DOI: 10.3389/fimmu.2018.01804.
- (61). Kothandan G; Gadhe CG; Cho SJ Structural Insights from Binding Poses of CCR2 and CCR5 with Clinically Important Antagonists: A Combined In Silico Study. *PLoS One* 2012, 7 (3), e32864 DOI: 10.1371/journal.pone.0032864.
- (62). da Fonseca TS; Silva GF; Guerreiro-Tanomaru JM; Sasso-Cerri E; Tanomaru-Filho M; Cerri PS Mast cells and immunoexpression of FGF-1 and Ki-67 in rat subcutaneous tissue following the implantation of Biodentine and MTA Angelus. *Int. Endod. J* 2019, 52 (1), 54–67 DOI: 10.1111/iej.12981. [PubMed: 29975794]
- (63). Sussman EM; Halpin MC; Muster J; Moon RT; Ratner BD Porous Implants Modulate Healing and Induce Shifts in Local Macrophage Polarization in the Foreign Body Reaction. *Ann. Biomed. Eng* 2014, 42 (7), 1508–1516 DOI: 10.1007/s10439-013-0933-0. [PubMed: 24248559]
- (64). Hotchkiss KM; Reddy GB; Hyzy SL; Schwartz Z; Boyan BD; Olivares-Navarrete R. Titanium surface characteristics, including topography and wettability, alter macrophage activation. *Acta Biomater.* 2016, 31, 425–434 DOI: 10.1016/j.actbio.2015.12.003. [PubMed: 26675126]

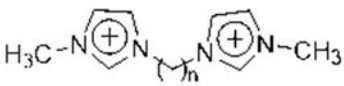
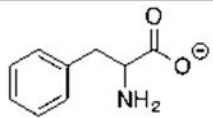
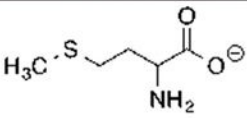
Ionic Liquids		
IonL-Phe	n = 10	
IonL-Met		

Figure 1.
Structures of ionic liquids used in this study.

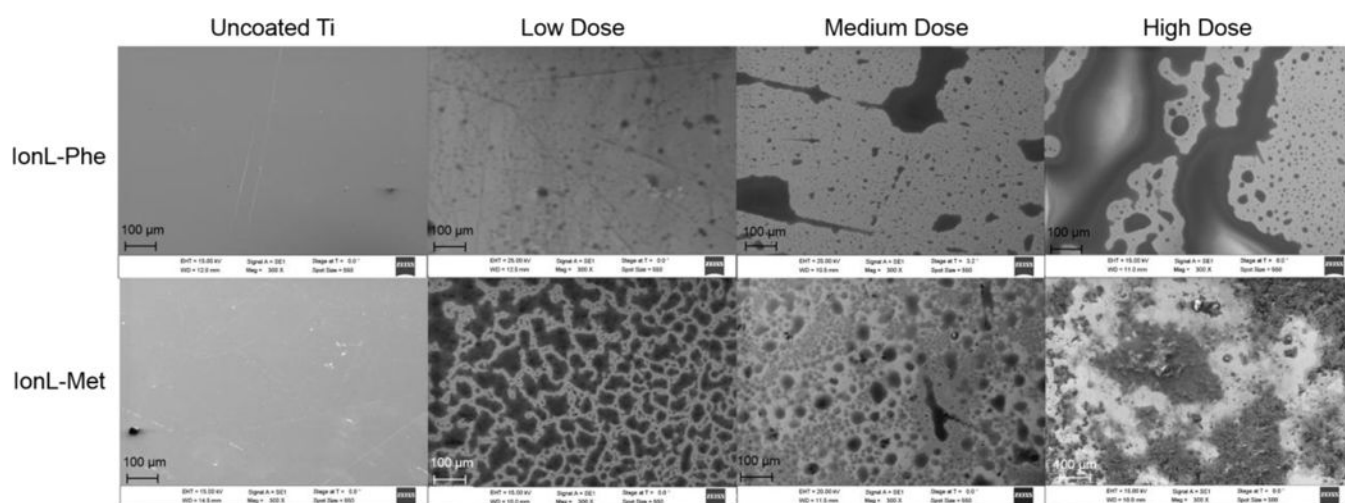


Figure 2.
SEM images illustrating ionic liquid coating behavior on titanium disks at different doses.

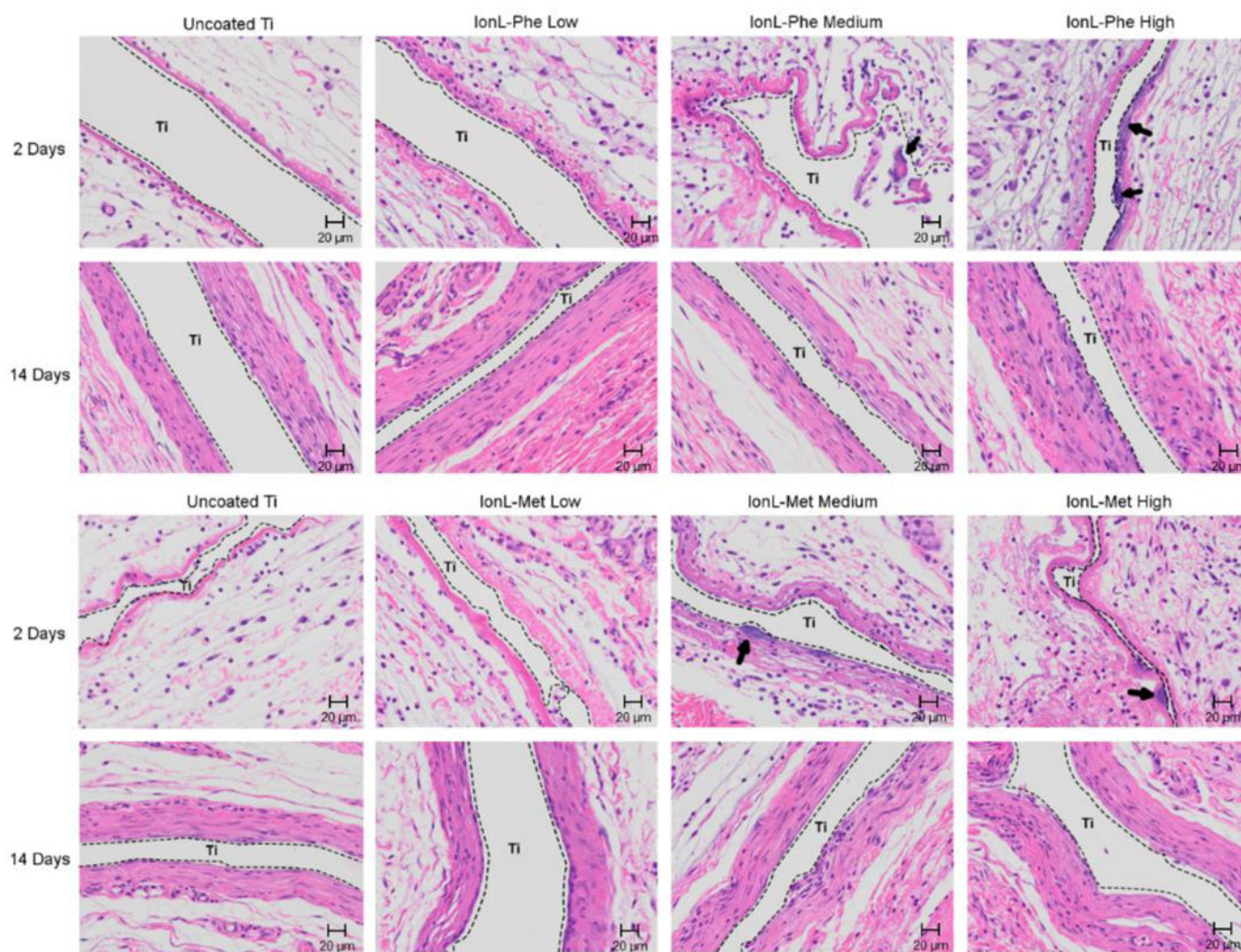


Figure 3.
Histology representing healing panel of uncoated and coated samples over time. H&E 20X.
Arrows indicate residual ionic liquid present on tissue.

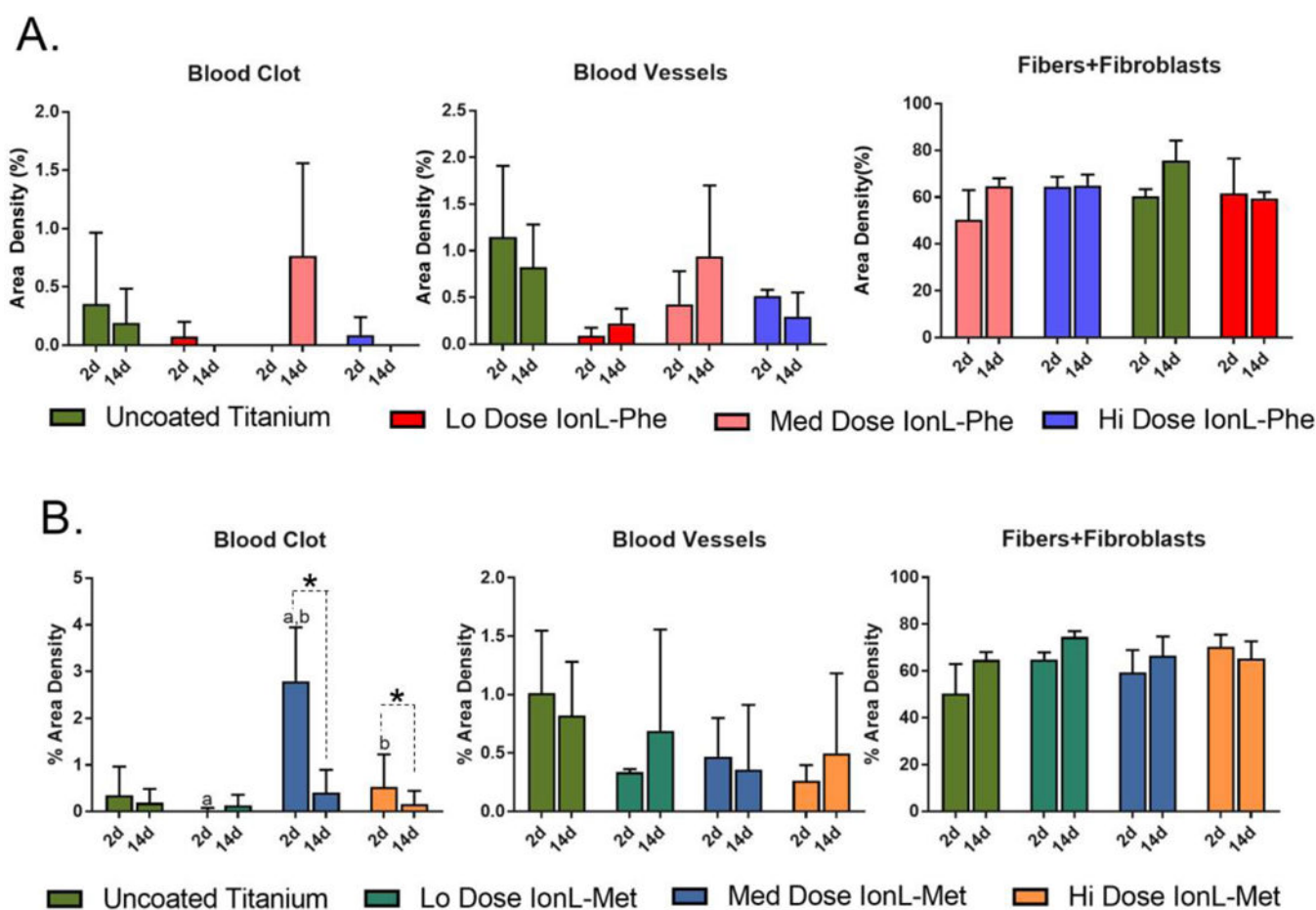


Figure 4.

Histomorphometry connective tissue parameters (blood clot, blood vessels, and fibers + fibroblasts) over time in uncoated and A. IonL-Phe and B. IonL-Met coated samples. * Indicates statistical significance between time points, while ^a and ^b indicate a difference between experimental groups, n=3 (p<0.05), error bars indicate standard deviation amongst means

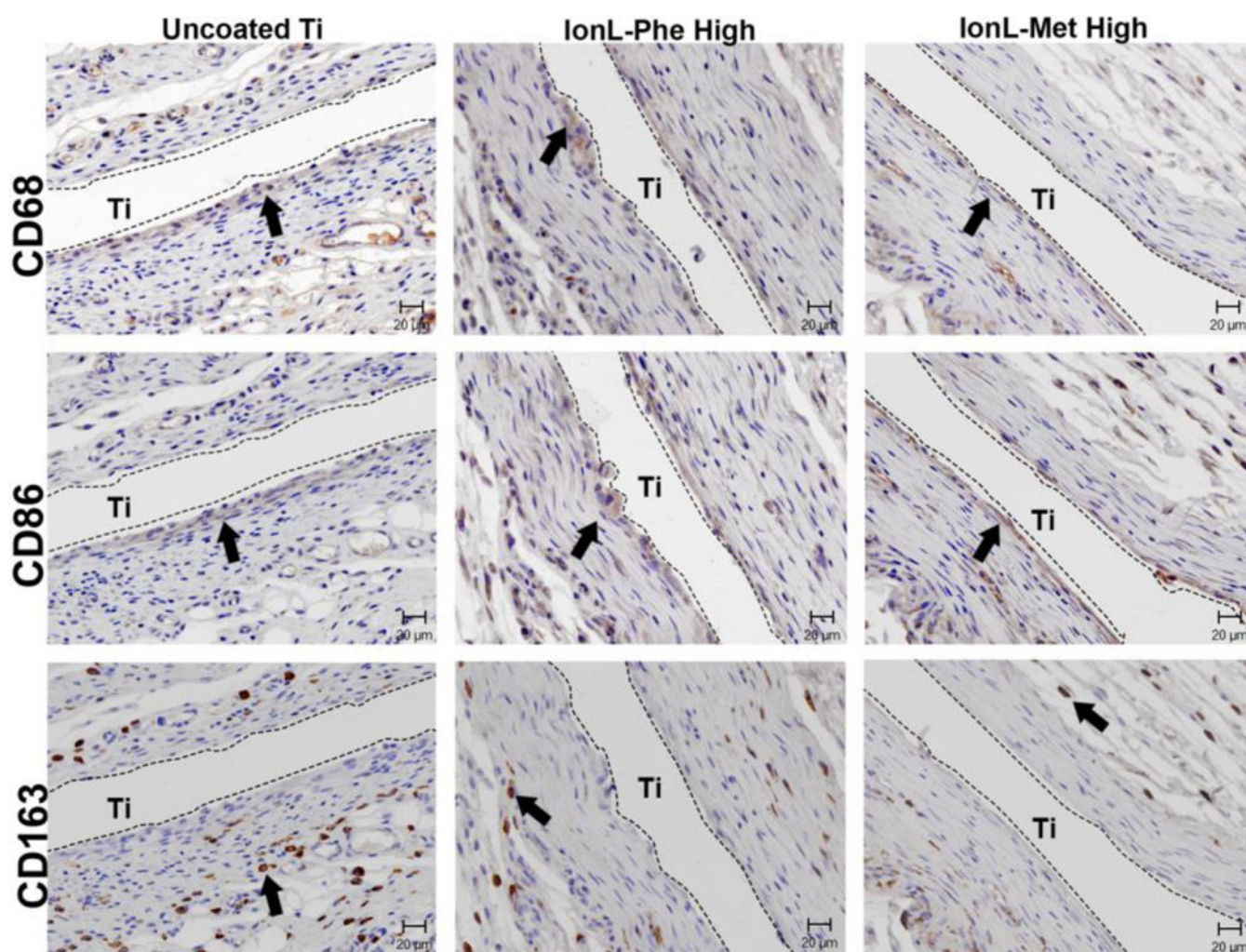


Figure 5. Immunohistochemistry (IHC) of CD68, CD86 and CD163 positive cells of Control (left) and Hi dose IonL-Met (right) at 14 days. Arrows indicated positively marked cells, * indicates histological artefacts, error bars indicated standard deviation amongst means.

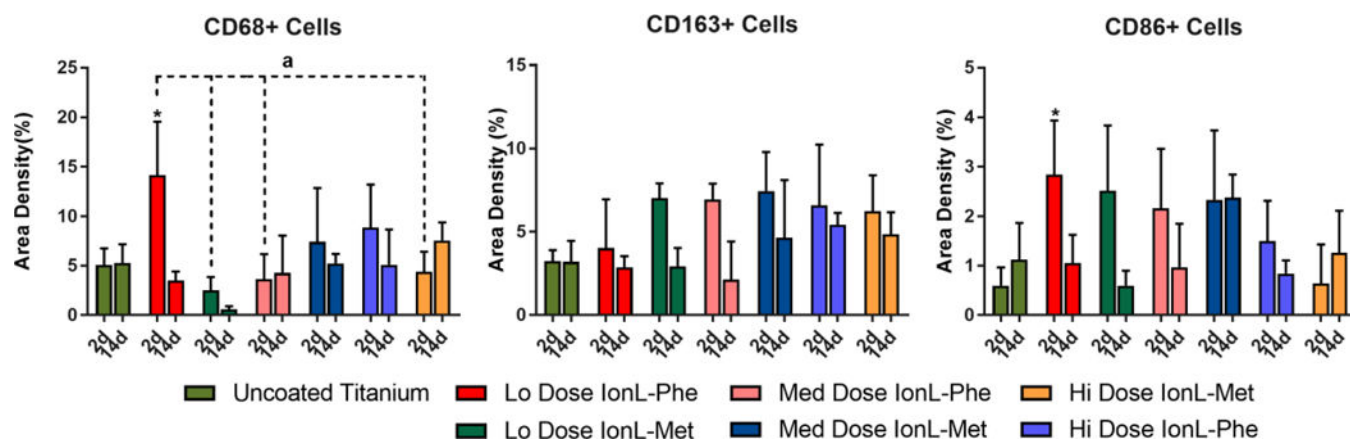


Figure 6. Immunohistochemistry (IHC) of macrophage surface markers over time in uncoated and coated samples. * Indicates statistical significance relative to uncoated control, while ^a indicates a difference between experimental groups, n=3 (p<0.05), error bars indicated standard deviation amongst means.

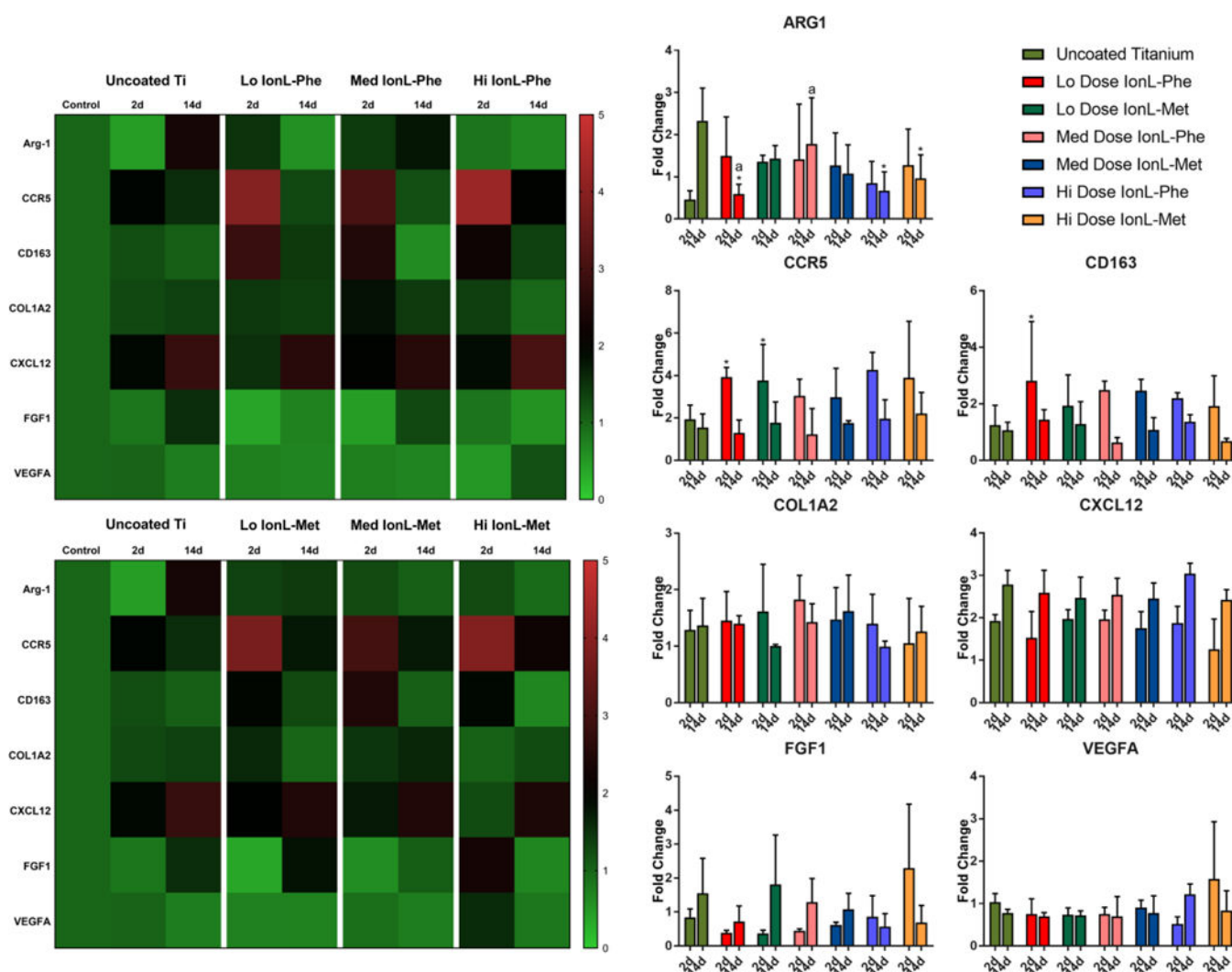


Figure 7. Heat map (left) depicting fold change of inflammatory and wound healing gene expression in uncoated and coated Ti relative to a non-surgery control, n=3. Bar graphs exhibiting the sample fold change divided by marker. * Indicates statistical significance relative to uncoated control, while ^a indicates a difference between experimental groups, n=3 (p<0.05), error bars indicated standard deviation amongst means.

Table 1.

Dip coating concentrations needed to achieve desired doses of IonL on specimens.

Ionic Liquid	IonL Concentration in Coating Solution (mM)	Amount of IonL on cpTi Disks after Drying (μmol)	Dose
IonL-Phe	305	1.0	High
IonL-Met	100	2.0	High
IonL-Phe	165	0.5	Medium
IonL-Met	50	1.0	Medium
IonL-Phe	50	0.1	Low
IonL-Met	9.0	0.2	Low